D. KALISZ*,# P.L. ŻAK*, T. TOKARSKI**, Ł. WZOREK***, J. S. SUCHY*, M. KICZOR*, W. CIEŚLAK*

COMPUTER SIMULATION OF THE FORMATION OF NON-METALLIC PRECIPITATES DURING A CONTINUOUS CASTING OF STEEL

The authors own computer software, based on the Ueshima mathematical model with taking into account the back diffusion, determined from the Wołczyński equation, was developed for simulation calculations. The applied calculation procedure allowed to determine the chemical composition of the non-metallic phase in steel deoxidised by means of Mn, Si and Al, at the given cooling rate. The calculation results were confirmed by the analysis of samples taken from the determined areas of the cast ingot. This indicates that the developed computer software can be applied for designing the steel casting process of the strictly determined chemical composition and for obtaining the required non-metallic precipitates.

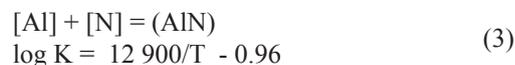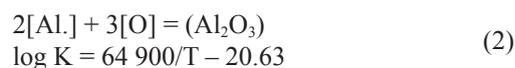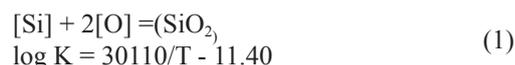*Keywords*: non-metallic oxide precipitates, modelling, continuous casting of steel, crystallization

1. Introduction

Non-metallic oxide precipitates are a negative product of refinery processes, and therefore should be efficiently removed from liquid steel. The main purpose of the oxides removal is lowering the oxide concentration in steel and obtaining the most favourable physical and chemical form of de-oxidation products. On the other hand, a small amount of fine oxide inclusions or their precipitation during crystallization processes can significantly influence the way in which the structure of the cast steel is formed. The positive effect of non-metallic oxides precipitates on the steel structure is principally related to their similar sizes, of 1 μm, and the uniform distribution within the metal volume [1-6]. This can happend when the precipitates are formed during the steel crystallization. Therefore prior to casting, the steel should contain an appropriate amount of oxygen needed for the precipitates formation. The mechanism of the oxide precipitates formation in the crystallization process can significantly help to regulate better the steel quality by controlling the size and distribution of non-metallic inclusions in the cast ingot [7-9].

2. Calculation procedure

The control over the chemical composition and size of the generated non-metallic precipitates is based on the cognition of the thermodynamic state of equilibrium of reactions between oxygen dissolved in liquid steel and chemical elements, chemically related to oxygen. The information concerning thermodynamic functions of components making up the metallic solution and non-metallic phase is crucial here. The thermodynamic functions change with the lowering temperature, which in turn affects the chemical composition of the precipitates. Another factor which strongly influences the chemical composition of precipitates is the liquid steel enrichment in dissolved elements: Al, Mn, Si, O and S on the crystallization front. This causes not only a gradual change of the composition of the precipitates, which evolve over the crystallization process, but also decreases the steel crystallization temperature. The scale of this effect depends on the cooling rate of steel during casting[1, 4, 10-12]. The most important precipitates are formed in steel according to the following reactions[1,4,10,11]:

$$[Si] + 2[O] = (SiO_2)$$
$$\log K = 30110/T - 11.40 \tag{1}$$

$$2[Al.] + 3[O] = (Al_2O_3)$$
$$\log K = 64\,900/T - 20.63 \tag{2}$$

$$[Al] + [N] = (AlN)$$
$$\log K = 12\,900/T - 0.96 \tag{3}$$

$$[Mn] + [S] = (MnS)$$
$$\log K = 8627/T - 4.745 \tag{4}$$

where: K – equilibrium constant of chemical reaction, T – temperature [K].

Computer calculations for de-oxidized steel with Mn, Si and Al, at the cooling rate of 50 K/min, were performed for determining the amount of non-metallic precipitates during continuous casting of steel. The simulation was based on

* AGH – UNIVERSITY OF SCIENCE AND TECHNOLOGY, FACULTY OF FOUNDRY ENGINEERING, AL. MICKIEWICZA 30, 30-059 KRAKÓW, POLAND

** AGH – UNIVERSITY OF SCIENCE AND TECHNOLOGY, ACADEMIC CENTER FOR MATERIALS AND NANOTECHNOLOGY, AL. A. MICKIEWICZA 30, 30-059 KRAKÓW, POLAND

*** AGH – UNIVERSITY OF SCIENCE AND TECHNOLOGY, FACULTY OF NON-FERROUS METALS, AL. MICKIEWICZA 30, 30-059 KRAKÓW, POLAND

Corresponding author: dak@agh.edu.pl

336

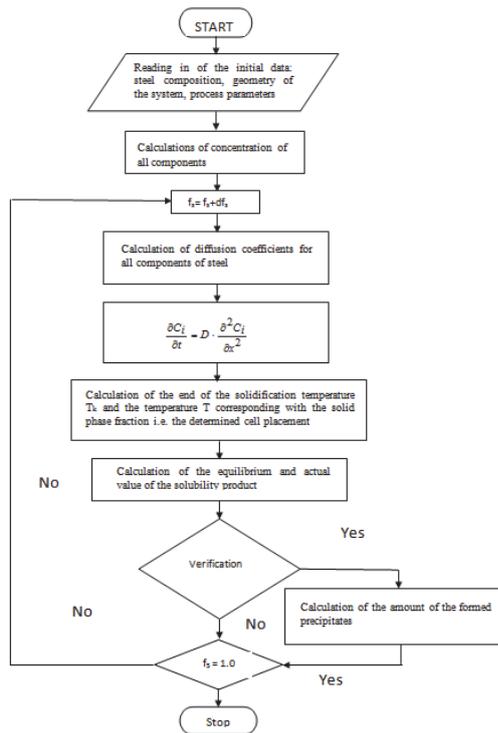a computer program, the block diagram of which is shown in Figure 1.

Fig. 1. Block diagram of computer program

The Ueshima mathematical model was used for modelling as it corresponds to the conditions of the directional heat removal during the dendritic crystallization [19,20]. In the case of δ phase crystallization, all components of the alloy tend to cluster in the liquid phase. Under these conditions the precipitates can be formed during the crystallization process [6-8, 13-18]. The concentration of component "i" of liquid steel on the crystallization front depends on the operation of two factors: the rate of advancement of the crystallization front and the diffusion rate of a component in the solid phase. The back diffusion effect takes place during crystallization, when part of the steel component joins the crystallization front and diffuses inside the crystal. The magnitude of the back diffusion effect on an individual component of liquid steel is characterized by the back diffusion parameter α_i.

$$\alpha_i = \frac{D_i \cdot t_s}{l^2} \tag{5}$$

The crystallization with diffusion was calculated by means of the Wołczyński equation [18]

$$C_S^* = k \cdot C_0 \cdot \left[1 + \alpha \cdot k \cdot f_S - f_S \right]^{\frac{k-1}{1-\alpha \cdot k}} \tag{6}$$

where: α_i – back diffusion parameter, D_i – diffusion coefficient

$[m^2 \cdot s^{-1}]$, l – distance [m], t_s – time [s], C_0 - initial concentration of solute in the liquid, C_S^* - concentration of a given solute in the solid phase, f_S- participation of solid phase (fraction of mass), k- equilibrium partition coefficient for solid/liquid phase interface.

The temperature dependences describing the diffusion coefficients and equilibrium division coefficients for steel components are given in Table 1 [1, 8]

TABLE 1

Diffusion coefficients in solid phase δ and equilibrium division coefficients of steel components

Chemical element	$D_\delta, \times 10^{-4} \frac{m^2}{s}$	$k^{\delta/L}$
Mn	0.76exp(-223472/RT)	0.77
S	4.56exp(-214443/RT)	0.05
Si	8exp(-248710/RT)	0.77
C	0.0127exp(-81301/RT)	0.19
P	2.9exp(--229900/RT)	0.23
Al	5.9exp(-241186/RT)	0.6
O	0.0371exp(-96349/RT)	0.03
N	0.008exp(-79078/RT)	0.32

where: L – liquid Fe, R – gas constant [J·mol⁻¹·K⁻¹], $k^{\delta/L}$ – equilibrium division coefficient.

3. Results of computer simulations

Calculations were performed under conditions of the thermodynamic equilibrium between the metallic liquid phase and non-metallic solid phase with the use of constant equilibriums of reactions during which MnO, SiO_2, Al_2O_3, MnS and AlN are formed [1, 4, 7, 10-12]. The chemical composition of the analyzed steel is presented in Table 2, and the results of computer simulations in Figures 2 – 7.
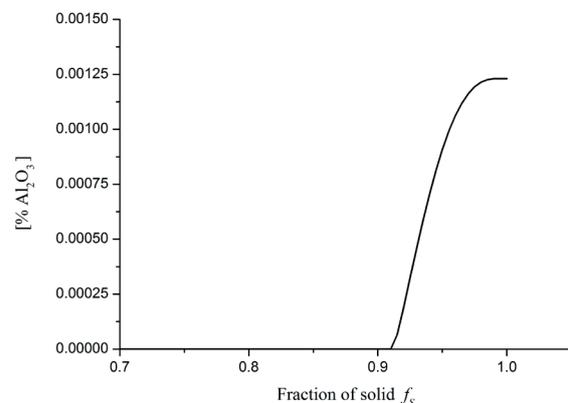

Fig. 2. Al_2O_3 content during S235 steel solidification at a cooling rate of 50 K/min

TABLE 2

Chemical composition of steel, wt.%

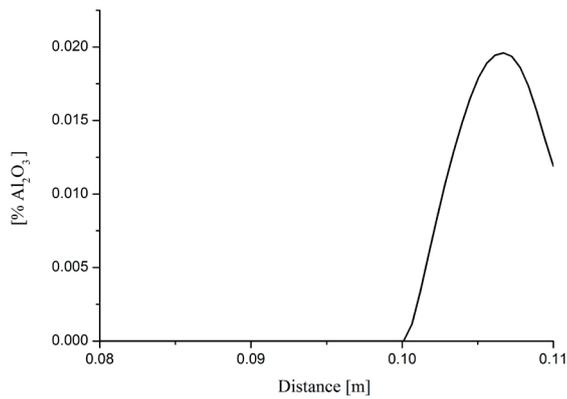| Type of steel	C	Mn	Si	P	S	Al	O	N
S235	0.08	0.78	0.017	0.013	0.01	0.07	0.0005	0.005

Fig. 3. Al_2O_3 content during S235 steel solidification at a cooling rate of 50 K/min (distance from the wall to the center of the ingot 0.11 m)
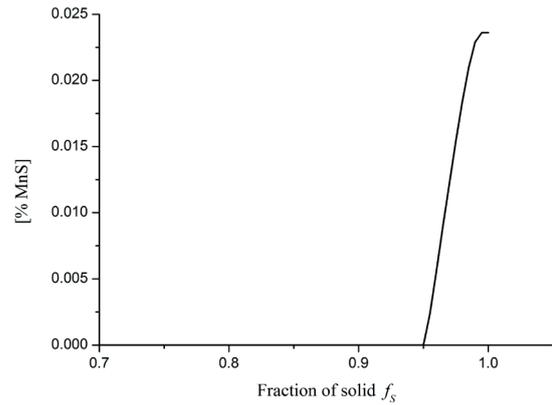

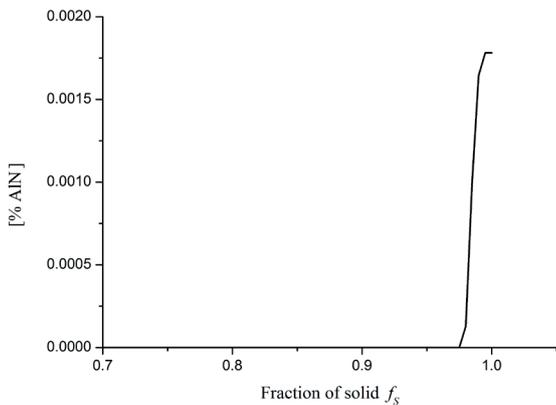Fig. 6. MnS content during S235 steel solidification at a cooling rate of 50 K/min

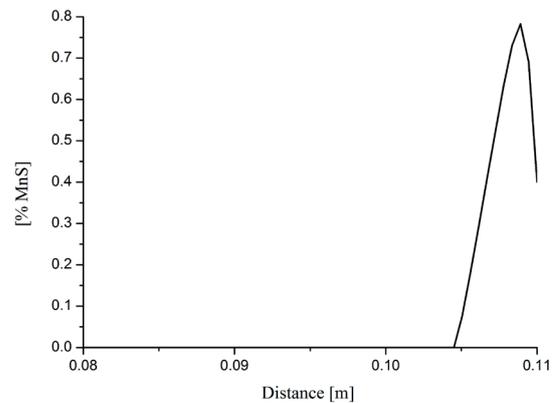Fig. 4. AlN content during S235 steel solidification at a cooling rate of 50 K/min

Fig.7. MnS content during S235 steel solidification at a cooling rate of 50 K/min (distance from the wall to the center of the ingot 0.11 m)
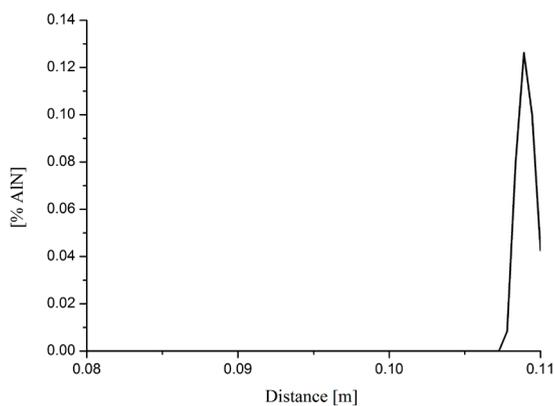

Fig. 5. AlN content during S235 steel solidification at a cooling rate of 50 K/min (distance from the wall to the center of the ingot 0.11 m)

4. Structure of cast steel

The microstructural analysis was performed for steel samples from the cast ingot 220 mm thick and 1500 mm wide. Apart from a preliminary identification, attempts were also made to establish the distribution of precipitates in a sample. The precipitates of the most diversified chemical composition and shape were searched for. The investigations were performed with the use of the SEM and X-ray microanalyses. The experiments were preceded by observation of samples in the optical microscope. Figures 8 to 10 illustrate the microstructure and distribution of precipitates in the steel sample collected from the central part of the ingot. Groups of tiny precipitates (Figs. 8 and 9) are presented in the microstructure (Fig. 11). The analysis of the X-ray microanalysis plots (Fig. 12) of the precipitates area (point 1) and the matrix (point 2) as well as the quantitative analysis results (Table 3) revealed that these precipitates could be identified as MnS. The precipitate composed of three particles is visible in the microstructure in Figure 13. The X-ray emission lines obtained from two different precipitates (points 1 and 2) (Fig. 14) as well as the results of quantitative analysis (Table 4) indicate the presence of clusters of MnS and Al_2O_3 precipitates.
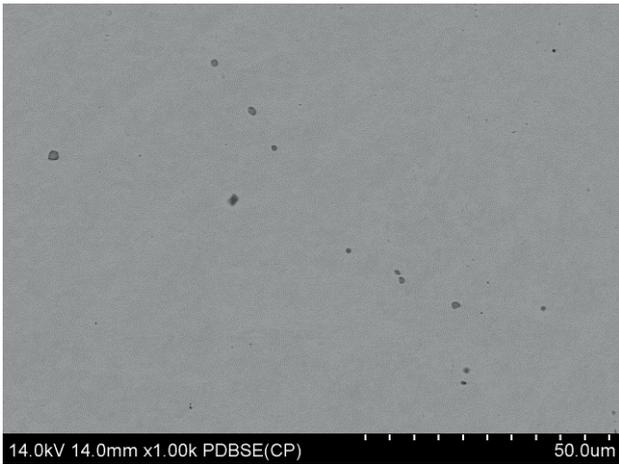
Fig. 8. The non-metallic precipitates distribution in the cast steel ingot (SEM)
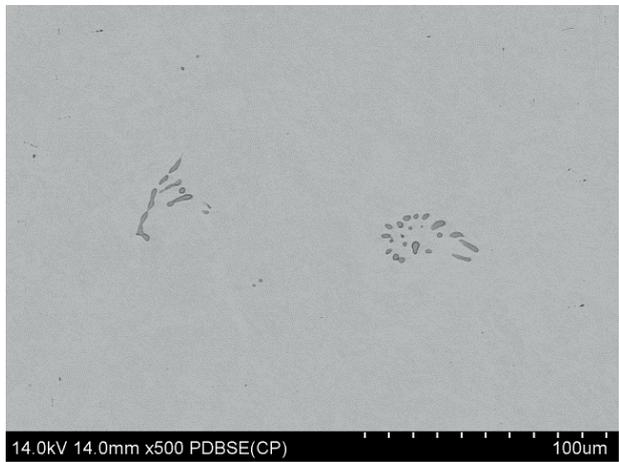

Fig. 9. The non-metallic precipitates distribution in the cast steel ingot (SEM)
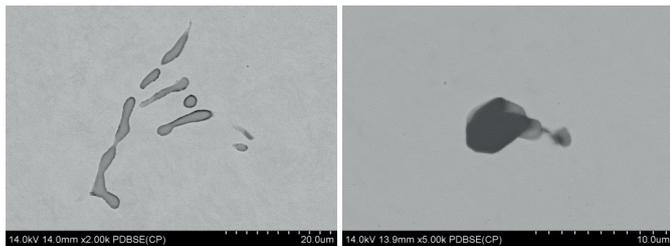

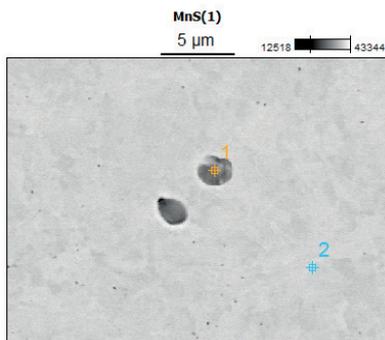Fig. 10. Morphology of the non-metallic precipitates from the cast steel ingot (SEM)

Fig. 11. Morphology and distribution of the non-metallic precipitates in the cast steel ingot
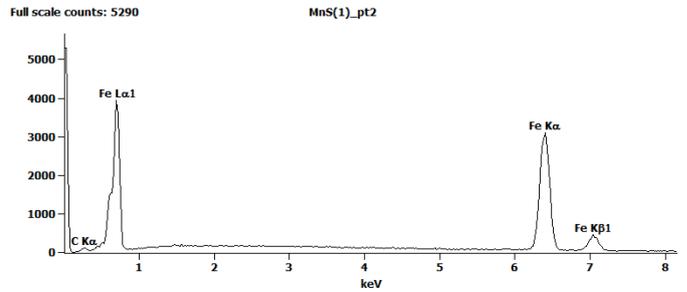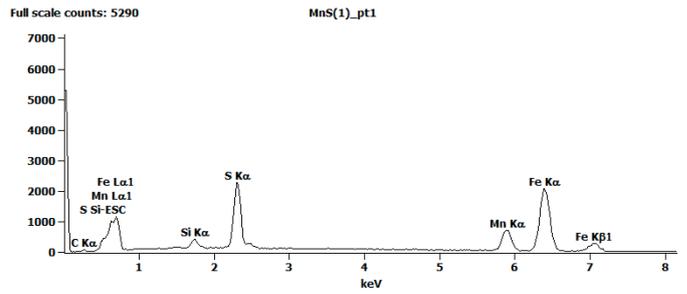

Fig. 12. EDS investigation obtained for the precipitate area (point 1) and the grid (point 2)

TABLE 3

Results of quantitative analysis obtained for the area of MnS precipitates (point 1) and the matrix (point 2)

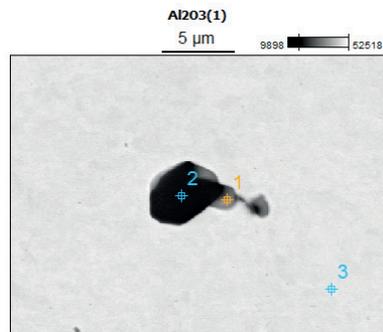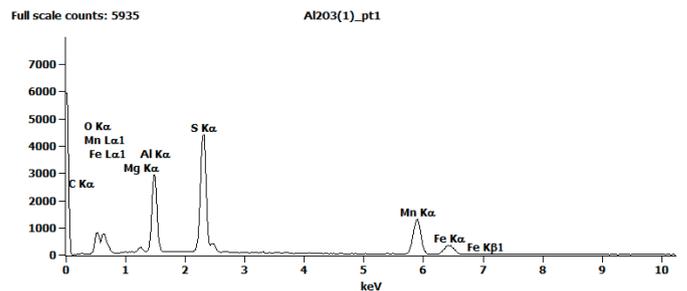| wt. %	C-K	Si-K	S-K	Mn-K	Fe-K
precipitate (pt 1)	1.53	1.28	10.20	18.83	68.16
matrix (pt 2)	1.36				98.64
atomic %	C-K	Si-K	S-K	Mn-K	Fe-K
precipitate (pt 1)	6.19	2.23	15.49	16.68	59.41
matrix (pt 2)	6.03				93.97

Fig. 13. Morphology and distribution of the non-metallic precipitates in the cast steel ingot (SEM)
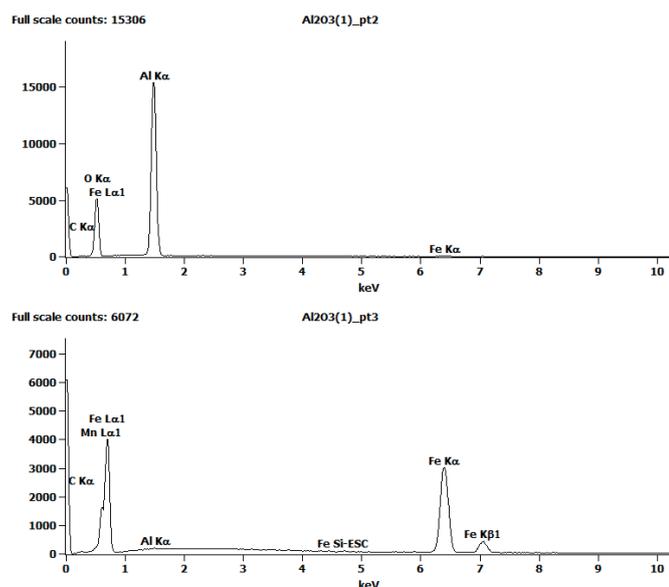
Fig. 14. EDS investigation obtained for the precipitate area (points 1 and 2) and the matrix (point 3)

The observations revealed that fine and irregular MnS precipitates dominate in the sample collected from the ingot. The Al_2O_3 particles were also identified. The latter takes the form of characteristic irregular spatial clusters. The statistical analysis of selected ingot areas was carried out to provide a more detailed identification and to determine the distribution of precipitates in a cross-section of the cast ingot. Five steel samples cut from various areas of the cast ingot were analyzed. The sampling places are presented in Figure 15.
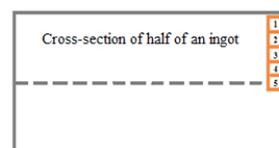

Fig. 15. Sampling places in the cast steel ingot

The statistical analysis of non-metallic precipitates in steel ingot was performed with the SEM method using the EDS detector and Thermo Scientific software. The advanced software module "Feature Sizing" was applied for the geometrical analysis of structural details and simultaneous chemical analysis. Having analyzed the picture obtained from the BSE detector and with the appropriately provided contrast threshold the authors could select elements of the structure, e.g. dark oxide precipitates. This created bases for determining areas of the material subjected to the subsequent chemical analysis. The measurements were performed individually for each determined area. Then the statistical analysis followed. It was based on ascribing individual particles definite sets on the basis of their geometrical and chemical identification. In the analyzed case, an area of 4.158 mm² was measured in each sample. The analyses covered 336 such areas at the 1000x magnification. The approximate duration of the analysis depended on the average number of particles classified for measurements, ranging from 1 to 4 hours. The obtained results of statistical analysis of precipitates in samples obtained for various areas (1 to 5) of the ingot are listed in Table 5.

The statistical analysis of the non-metallic precipitates distribution in the ingot reveals that during crystallization

TABLE 4

Results of quantitative analysis for the area of MnS and Al_2O_3 precipitates (points 1 and 2) and the matrix (point 3)

wt %	C-K	O-K	Mg-K	Al-K	S-K	Mn-K	Fe-K
precipitate (pt 1)	1.99	5.95	0.83	13.41	23.90	44.02	9.90
precipitate (pt 2)	1.48	45.15		51.65			1.72
matrix (pt 3)	0.88			0.23		0.63	98.26
atomic %	C-K	O-K	Mg-K	Al-K	S-K	Mn-K	Fe-K
precipitate (pt 1)	5.93	13.31	1.22	17.79	26.69	28.69	6.35
precipitate (pt 2)	2.52	57.70		39.14			0.63
matrix (pt 3)	3.94			0.45		0.62	94.98

TABLE 5

Distribution of non-metallic precipitates in samples (1 to 5) collected from the cast steel ingot

Parameters	1	2	3	4	5
Number of particles of non-metallic precipitates	663	640	396	123	6
Surface area of non-metallic precipitates [μm2]	3264.96	4964.11	1277.05	1602.01	12.02
Area of MnS [μm2]	173.030	2588.400	520.600	147.460	12.02
Number of MnS precipitates	85	377	201	76	6
Area of Al_2O_3 [μm2]	201.070	128.020	86.560	78.640	1.380
Number of Al_2O_3 precipitates	42	15	13	15	1
Area of SiO_2 [μm²]	99.370	17.060	53.440	80.270	0
Number of SiO_2 precipitates	45	10	19	10	0

340

of steel mainly the MnS and Al_2O_3 precipitates are formed. Samples 1 and 2 contain the highest number of precipitates. These are non-metallic particles which did not manage to outflow and be assimilated by crystallizer slag, and which acting with the crystallization front, were absorbed by it. Steel samples collected from the central part of the ingot contain trace amounts of precipitates. Such distribution of non-metallic particles can be a result of good mixing of steel in the crystallizer, e.g. by the magnetic mixer.

5. Concluding remarks

The results of computer simulation were confirmed experiments performed by means of microscopic techniques carried out for the analyzed type of steel, where Al_2O_3 and MnS precipitates were observed to be formed. The differences related to the presence of these precipitates in samples are indicative of primary precipitates and products of refining processes, which entered the crystallizer with liquid steel. The computer simulations performed by the authors were made only for secondary precipitates. The content of oxygen dissolved in steel to be cast, ranges between 3 and 5ppm, signifying that the amount of oxides precipitated during the crystallization process is low. The ultimately low oxygen content in steel hinders the formation of SiO_2 precipitates. The SiO_2 precipitates identified by microscopic analyses are primary ones, i.e. they were present in liquid steel and were not a consequence of precipitation processes taking place during the crystallization. Hence the conclusion that it is necessary to leave some amount of non-metallic oxide precipitates (products of refining of steel) to form a fine structure of steel. The remaining non-metallic phases: sulphides and nitrides will also play an important role in this process.

Received: 10 March 2015.

REFERENCES

[1] D. Kalisz, Termodynamiczna Charakterystyka Powstawania Fazy Niemetalicznej w Ciekłej Stali, Wyd. Naukowe Akapit (2013).

[2] J. M. Gregg, H. K. Bhadeshia, Acta Materialia **45,** 739-748 (1979).

[3] M. Ohta, N. Sano, K. Morita, ISIJ Int. **40**, 87-91 (2000).

[4] M. Suzuki, R. Yamaguchi, K. Murakami, M. Nakada, ISIJ Int. 41 (2001).

[5] J. Iwanciw, D. Podorska, J. Wypartowicz, Archives of Metallurgy and Materials **56**, 4 (2011).

[6] D. Kalisz, P. L. Żak, Archives of Metallurgy and Materials **59**, 4 (2014).

[7] D. Kalisz, P. L. Żak, Kovove Mater. **53**, 1 (2015).

[8] D. Kalisz, P. L. Żak, J. Lelito, M. Szucki, J. S. Suchy, B. Gracz, Metallurgy **54,** 1(2015).

[9] S. Kobayashi, ISIJ Int. 39 (1999).

[10] Z. Morita, T. Tanaka, T. Yanai, Met. Trans. B, **18**B (1987).

[11] Z. Liu, K. Gu, K. Cai, ISIJ Int. 42 (2002).

[12] T. Matsumiya, H. Kajioka, S. Mizoguchi, Y. Ueshima, H. Esaka, ISIJ Int. 24 (1984).

[13] Y. Ueshima, S. Mizoguchi, T. Matsumiya, H. Karioka, Met. Trans. B, **17**B (1986).

[14] Z. Ma, D. Janke ISIJ Int. 38 (1998).

[15] Z. Liu, J. Wei, K. Cai, ISIJ Int. 42 (2002).

[16] T.W. Clyne, W. Kurz, Met. Trans. A, **12**A (1981).

[17] I. Ohnaka ISIJ Int. 26 (1986).

[18] W. Wołczyński, Effect of the Back Diffusion onto Doublet Structure Formation and Solute Redistribution Within Alloys Solidyfying Directionally, With Or Without Convection, Polish Academy of Science, Krakow (2002).